JOURNAL OF NATURAL PRODUCTS

pubs.acs.org/jnp Article

Phenolic Constituents of the Roots of *Rhamnoneuron balansae* with Senolytic Activity

Hyo-Moon Cho, Yae-Rin Lee, Ba-Wool Lee, Mi Zhang, Byeol Ryu, Du-Trong Nghiem, Ha-Thanh-Tung Pham, and Won-Keun Oh*

Cite This: https://dx.doi.org/10.1021/acs.jnatprod.0c00885 Read Online

ABSTRACT: With the advent of senolytic agents capable of selectively removing senescent cells in old tissues, the perception of age-associated diseases has been changing from being an inevitable to a preventable phenomenon of human life. In the search for materials with senolytic activity from natural products, six new flavonostilbenes (**1**−**6**), three new phenylethylchromanones (**7**−**9**), three new phenylethylchromones (**10**−**12**), and four known compounds (**13**−**16**) were isolated from the roots of *Rhamnoneuron balansae*. The chemical structures of these isolated compounds were determined based on the interpretation of spectroscopic data, including 1D and 2D NMR, ECD, and HRMS. The absolute configuration of compound **1** was also determined by a Mosher ester analysis and ECD calculations. Compounds **6**−**8** were shown to selectively destroy senescent cells, and the promoter activity of p16INK4A, a representative senescence marker, was reduced significantly by compound **6**. The present results suggest the potential activity of flavonostilbene and phenylethylchromanone skeletons from *R. balansae* as new senolytics.

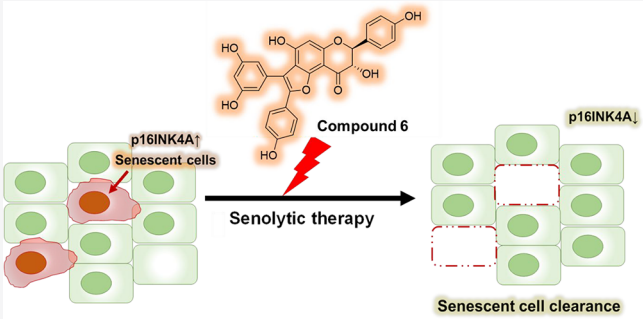

The average life expectancy for people born in the U.S. in 1959 has risen from 69.9 years to 78.9 years,[1] which is attributed to improved medical care, knowledge of hygiene, and access to vaccinations. The U.S. and other wealthy countries have kept pace with this tendency over the past few decades. However, since a prolonged life span is not always proportional to an individual's health, interest has grown as to how to age well by preserving physical and mental health to maximize the quality of life during one's elderly years.[2] Aging accompanies the progressive accumulation of structural and functional damage in an organism and is prone to result in multiple and serious chronic diseases, including Alzheimer's disease, osteoporosis, diabetes, frailty, and lung diseases.[3] Thus, many researchers have investigated fundamental aging mechanisms, which include cellular senescence.

Cellular senescence is a state in which cells cannot permanently replicate but are viable metabolically and triggered by various stimuli, including DNA damage (e.g., telomere shortening), reactive oxygen species (ROS) generation, and oncogenes (e.g., Ras and Myc).[4] Senescent cells are characterized by particular morphological and metabolic changes, including enlarged cell shapes and resistance against apoptosis, chromatin reorganization, altered gene expression, and the acquisition of the senescence-associated secretory phenotype (SASP), including proinflammatory cytokines, bradykinins, chemokines, proteases, and miRNAs.[5] Senescent cells accumulate in various tissues, and the secretion of SASP by these aged cells causes chronic inflammation in normal cells, ultimately resulting in tissue damage and immune system disturbance.[6] To overcome this chronic senescence, anti-senescent drugs have been presented as "senolytics" that specifically eliminate senescent cells by inducing apoptosis and "senomorphics" that can suppress senescence indirectly by SASP inhibition.[7] During cell cycle arrest, the p53/p21^{WAF1} axis and p16INK4A play their roles in the initiation of senescence and the maintenance of state, respectively.[8] Proteins of the B-cell lymphoma 2 (BCL-2) family, ephrin-dependent receptors, HSP90, PI3Kδ/Akt, and FOXO4a/p21, which comprise the senescent cell antiapoptotic pathways (SCAPs), have been suggested to be involved in apoptosis resistance.[9] As SASP inhibitors, many studies on the related pathways of NF-κB, mTOR, and p38MAPK have been proposed.[10] Dasatinib (an inhibitor of the Eph receptors), quercetin (a modulator of several pathways, such as NF-κB and mTOR), navitoclax (an inhibitor of the BCL-2 family proteins), and fisetin are reported to have senolytic activity.[11−14] Apigenin and kaempferol, rapamycin (a specific inhibitor of mTOR), and ruxolitinib (a JAK inhibitor) have

Received: August 8, 2020

been suggested to be interesting senomorphics.[15−18] Recently, promising results have been reported in several clinical studies where a combined treatment of dasatinib and quercetin significantly reduced SASP factors and the burden of senescent cells. Thus, research is starting to find senotherapeutics from natural resources with favorable safety profiles.[19]

Rhamnoneuron balansae (Drake) Gilg is a medium-sized tree belonging to the family Thymelaeaceae and is distributed throughout northern Vietnam and mainland China. The plant has been utilized as a raw material for Dó paper, also known as bamboo paper, and has been used in traditional Vietnamese crafts for centuries. Dó paper exhibits no smudging of ink, is resistant to moisture and acid, and offers protection from termites. The durability of this paper makes it an important source for folk crafts. Despite being used for centuries, little has been reported about its chemical constituents, including studies on its pharmacological activity.[20] Herein are reported the isolation and structure determination of 12 new compounds from a 70% ethanol extract of the roots of *R. balansae*. In addition, the pharmacological activity of *R. balansae* and its constituents was investigated, and rhamnoneuronal C (**6**) and balansechromanones A (**7**) and B (**8**) were found to be potential senolytic candidates.

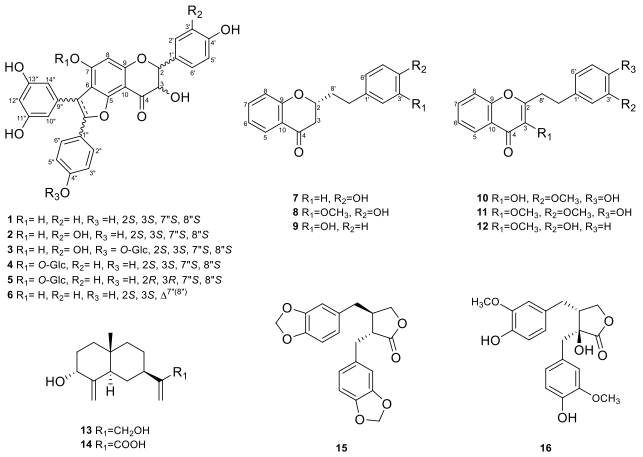

■ RESULTS AND DISCUSSION

A 70% ethanol extract of the dried roots of *R. balansae* was applied to a series of chromatographic techniques, including passage over silica gel, reversed-phase-C_{18}, and Sephadex LH-20. Subsequently, preparative high-performance liquid chromatography (HPLC) was applied to obtain six flavonostilbenes (**1**−**6**), three phenylethylchromanones (**7**−**9**), and three phenylethylchromones (**10**−**12**) along with four known compounds (**13**−**16**).

Compound **1**, obtained as a light yellow, amorphous powder with $[\alpha]_D^{25}$ −15 (*c* 0.1, MeOH), was found to possess a molecular formula of $C_{29}H_{22}O_9$, based on the high-resolution electrospray ionization mass spectrometry (HRESIMS) ion peak at *m/z* 513.1192 $[M - H]^-$ (calcd for $C_{29}H_{21}O_9$, 513.1191). The IR data exhibited the absorption of hydroxy (3375 cm^{-1}) and carbonyl (1659 cm^{-1}) functionalities. The ^1H NMR spectrum (Table 1) displayed signals for one aromatic methine proton at δ_H 5.98 (1H, s), four sets of protons from two 1,4-disubstituted benzene moieties at δ_H 7.38, 7.19, 6.84, and 6.79 (each 2H, d, *J* = 8.6 Hz), three aromatic protons from one 1,3,5-trisubstituted benzene moiety at δ_H 6.10 (2H, d, *J* = 2.0 Hz) and 6.15 (1H, d, *J* = 2.1 Hz), two methines of a dihydroflavonol moiety at δ_H 5.02 and 4.47 (each 1H, d, *J* = 11.6 Hz), and two methines of a dihydrobenzofuran moiety at δ_H 5.52 and 4.29 (each 1H, d, *J* = 5.1 Hz). The ^{13}C NMR data (Table 3) showed all 29 expected carbon resonances. Fifteen of the carbon signals were explained by a dihydrokaempferol skeleton, including four oxygenated aromatic carbons and one carbonyl carbon at δ_C 159.1, 163.0, 163.5, 165.2, and 192.9. The remaining 14 carbon signals suggested the presence of the fused stilbene moiety ($C_6-C_2-C_6$) by heteronuclear multiple bond correlations (HMBC) (Figure 1). The HMBC correlations between H-2′/6′ (δ_H 7.38, 6.84) and C-2 (δ_C 84.9) and of H-8 (δ_H 5.98) and C-6 (δ_C 111.1), C-7 (δ_C 163.0), C-9 (δ_C 165.2), and C-10 (δ_C 100.8) showed the presence of dihydroflavonol with a 1,4-disubstituted B-ring. A 1,2-diaryl-dihydrobenzofuran ring containing 1,4-disubstituted and 1,3,5-trisubstituted benzene rings was suggested by the HMBC correlations from H-7″ (δ_H 5.52) to C-1″ (δ_C 133.3) and C-2″/6″ (δ_C 128.2), as well as from H-8″ (δ_H 4.29) to C-9″ (δ_C 146.2) and C-10″/14″ (δ_C 106.7). The linkage of the resveratrol and dihydrokaempferol moieties was confirmed by the HMBC correlations from H-7″ to C-5 (δ_C 163.5) and C-6 and from H-8″ to C-5, C-6, and C-7. The relative configuration of compound **1** were assigned all-*trans* orientations by the nuclear Overhauser effect spectroscopy (NOESY) correlations (Figure 2A and B) between H-3 and H-2′/6′, H-7″ and H-10″/14″, and H-8″ and H-2″/6″, respectively. These assignments were supported by the large $J_{2,3}$ value of 11.6 Hz and the small $J_{7'',8''}$ value of 5.1 Hz in comparison to those from previous studies.[21−23] The absolute configurations of C-2 and C-3 were determined as 2*S*,3*S* based on Mosher ester analysis (Figures S94−97 and Table S1, Supporting Information).[24] Moreover, the remaining absolute configuration of the dihydrobenzofuran moiety was assigned by a comparative analysis of the experimental electronic circular dichroism (ECD) spectra using the time-dependent density functional theory (TDDFT) method at the 6-31G/B3LYP level (Figure 3A). By considering the molecular orbital transitions and comparing the experimental data with the calculated data, the absolute configuration of **1** was suggested as 2*S*,3*S* based on a negative n → π* Cotton effect (CE) of 300−340 nm and 7″*S*,8″*S* based on a negative CE of 240 nm (Figure S101 and Table S24, Supporting Information). From all of the aforementioned observations, the absolute configuration of compound **1** was defined as 2*S*,3*S*,7″*S*,8″*S*, and this compound was named rhamnoneuronal A.

Compound **2** (rhamnoneuronal B) was isolated as a pale yellow, amorphous powder with $[\alpha]_D^{25}$ −52 (*c* 0.1, MeOH). The molecular formula, $C_{29}H_{22}O_{10}$, was established from the $[M - H]^-$ HRESIMS ion at *m/z* 529.1117 (calcd for $C_{29}H_{21}O_{10}$, 529.1140). The IR spectrum exhibited absorption bands of hydroxy (3357 cm^{-1}) and carbonyl (1612 cm^{-1}) functionalities. The ^1H and ^{13}C NMR data (Tables 1 and 3) displayed features similar to those of **1**, except for the B-ring of the dihydroflavonol unit. The 1D NMR spectra of **2** showed that the B-ring of the dihydrokaempferol of **1** was replaced with a dihydroquercetin unit from the correlations between H-2′ at δ_H 6.99 (1H, d, *J* = 2.0 Hz; δ_C 115.9), H-5′ at δ_H 6.81 (1H, d, *J* = 8.1 Hz; δ_C 116.1), and H-6′ at δ_H 6.87 (1H, dd, *J* = 8.1, 2.0 Hz; δ_C 120.9). The absolute configuration of **2** was defined as 2*S*,3*S*,7″*S*,8″*S* through comparative analysis with the spectroscopic data of compound **1**, including the coupling

https://dx.doi.org/10.1021/acs.jnatprod.0c00885
J. Nat. Prod. XXXX, XXX, XXX−XXX

Table 1. NMR Spectroscopic ^{1}H NMR Data for Compounds 1−6

	1[b]	2[b]	3[b]	4[b]	5[b]	6[b]
position	δ_H (J in Hz)	δ_H (J in Hz)	δ_H (J in Hz)	δ_H (J in Hz)	δ_H (J in Hz)	δ_H (J in Hz)
2	5.02, d (11.6)	4.95, d (11.5)	5.02, d (11.6)	5.07, d (11.7)	5.06, d (11.8)	5.10, d (11.9)
3	4.47, d (11.6)	4.42, d (11.5)	4.48, d (11.6)	4.53, d (11.7)	4.57, d (11.8)	4.60, d (11.9)
8	5.98, s	5.98, s	5.98 s	6.35, s	6.35, s	6.20, s
2′	7.38, d (8.6)	6.99, d (2.0)	7.38, d (8.5)	7.38, d (8.5)	7.39, d (8.5)	7.41, d (8.5)
3′	6.84, d (8.6)		6.85, d (8.5)	6.84, d (8.5)	6.84, d (8.5)	6.86, d (8.5)
4′						
5′	6.84, d (8.6)	6.81, d (8.1)	6.85, d (8.5)	6.84, d (8.5)	6.84, d (8.5)	6.86, d (8.5)
6′	7.38, d (8.6)	6.87, dd (8.1, 2.0)	7.38, d (8.5)	7.38, d (8.5)	7.39, d (8.5)	7.41, d (8.5)
1″						
2″	7.19, d (8.6)	7.18, d (8.5)	7.31, d (8.7)	7.18, d (8.5)	7.14, d (8.6)	7.45, d (8.8)
3″	6.79, d (8.6)	6.79, d (8.5)	7.13, d (8.7)	6.79, d (8.5)	6.78, d (8.6)	6.71, d (8.8)
4″						
5″	6.79, d (8.6)	6.79, d (8.5)	7.13, d (8.7)	6.79, d (8.5)	6.78, d (8.6)	6.71, d (8.8)
6″	7.19, d (8.6)	7.18, d (8.5)	7.31, d (8.7)	7.18, d (8.5)	7.14, d (8.6)	7.45, d (8.8)
7″	5.52, d (5.1)	5.52, d (5.2)	5.58, d (5.0)	5.62, d (5.6)	5.65, d (5.2)	
8″	4.29, d (5.1)	4.28, d (5.2)	4.27, d (5.0)	4.33, d (5.6)	4.32, d (5.2)	
9″						
10″	6.10, d (2.0)	6.10, d (2.2)	6.11, d (2.1)	6.14, d (2.1)	6.15, d (2.1)	6.38, d (2.2)
11″						
12″	6.15, t (2.1)	6.15, t (1.6)	6.16, t (2.2)	6.17, t (2.1)	6.16, t (2.1)	6.30, t (1.8)
13″						
14″	6.10, d (2.0)	6.10, d (2.2)	6.11, d (2.1)	6.14, d (2.1)	6.15, d (2.1)	6.38, d (2.2)
Glc						
1‴			4.93, d (7.5)	4.85, d[d]	4.88, d[d]	
2‴			3.46, m[d]	3.20, dd (9.0, 7.9)	3.22, dd (9.0, 7.9)	
3‴			3.44, m[d]	3.34, t (9.1)	3.30, t (9.1)	
4‴			3.39, m[d]	3.30, t (9.2)	3.00, t (9.2)	
5‴			3.46, m[d]	3.37, m	3.35, m	
6‴			3.91, dd (12.1, 5.7)[f]	3.81, dd (12.1, 2.0)	3.83, dd (12.1, 2.1)	
			3.72 dd (12.1, 2.2)	3.62, dd (12.1, 5.5)	3.64, dd (12.1, 5.3)	

[a]Recorded in methanol-d_4 at 400 MHz. [b]Recorded in methanol-d_4 at 800 MHz. [c]Recorded in $CDCl_3$ at 800 MHz. [d]Overlapped.

constants, a NOESY experiment, and the ECD spectrum (Figure 3B). Accordingly, compound **2** was assigned as shown.

Compound **3** (rhamnoneuroside A) was obtained as a light yellow, amorphous powder with $[\alpha]_D^{25}$ −98 (c 0.1, MeOH). The molecular formula, $C_{35}H_{32}O_{14}$, was established from the deprotonated HRESIMS ion peak at m/z 675.1716 (calcd for $C_{35}H_{31}O_{14}$, 675.1714). The IR spectrum exhibited absorption bands for hydroxy (3389 cm^{-1}) and carbonyl (1600 cm^{-1}) functionalities. The NMR data of compound **3** were very similar to those of **2** except for the presence of a β-D-glucose moiety. The β-glucopyranosyl unit was deduced through a large coupling constant of the anomeric proton at δ_H 4.93 (1H, d, J = 7.5 Hz; δ_C 102.2), and the connectivity of six protons appearing in the aliphatic region was revealed by the ^{1}H−^{1}H COSY experiment. The HMBC correlation between H-1‴ (δ_H 4.93) and C-4″ (δ_C 159.1) suggested that the glucose group in compound **3** is attached to C-4″ of the stilbene moiety. The absolute configuration of compound **3** (2*S*,3*S*,7″*S*,8″*S*) was assigned through a comparative ECD analysis (Figure 3B). Accordingly, the structure of compound **3** was determined as shown.

Compound **4** (rhamnoneuroside B) was isolated as a light yellow, amorphous powder with $[\alpha]_D^{25}$ −140 (c 0.1, MeOH). The molecular formula, $C_{35}H_{32}O_{14}$, was established from the $[M - H]^-$ HRESIMS ion peak at m/z 675.1724 (calcd for $C_{35}H_{31}O_{14}$, 675.1719). The IR spectrum exhibited absorption bands for hydroxy (3347 cm^{-1}) and carbonyl (1616 cm^{-1}) functionalities. A comparison of the 1D and 2D NMR data of **1** with **4** showed that the additional signals of an anomeric proton at δ_H 4.85 (1H, d), corresponding to the carbon resonance at δ_C 101.3, indicated the presence of a β-D-glucose moiety. The HMBC correlation between H-1‴ of glucose and C-7 suggested that the glucose residue is located at C-7 of a dihydrokaempferol moiety. The absolute configuration of compound **4** (2*S*,3*S*,7″*S*,8″*S*) was defined through the close similarity of the ECD curve with that of compound **1**. Consequently, compound **4** was assigned as shown.

Compound **5** (rhamnoneuroside C) was obtained as a light yellow, amorphous powder with $[\alpha]_D^{25}$ −45 (c 0.1, MeOH). The molecular formula of **5** was determined as $C_{35}H_{32}O_{14}$ from the $[M - H]^-$ HRESIMS ion peak at m/z 675.1716 (calcd for $C_{35}H_{31}O_{14}$ 675.1714). The IR spectrum exhibited absorption bands for hydroxy (3361 cm^{-1}) and carbonyl (1617 cm^{-1}) groups. The NMR spectra of **5** were very similar to those of **4**, whereas the respective ECD analysis of compounds **4** and **5** indicated them to be diastereoisomers. The key rotating-frame Overhauser enhancement spectroscopy (ROESY) correlations (Figure 2A and C) between H-3 and H-2′/6′ and the large coupling constant ($J_{2,3}$) showed that the relative configuration of H-2 and H-3 of **5** is the same as in compound **4** with a *trans* conformation. However, the positive n → π^* CE at 300−340 nm of compound **5** suggested that the absolute configuration of the dihydrokamferol unit appeared different from that of **4** (Figure 3C).[25] Therefore, the absolute

https://dx.doi.org/10.1021/acs.jnatprod.0c00885
J. Nat. Prod. XXXX, XXX, XXX−XXX

Table 2. NMR Spectroscopic ^{1}H NMR Data for Compounds 7−10

	7[a]	8[a]	9[a]	10[b]	11[c]	12[c]
position	δ_H (J in Hz)	δ_H (J in Hz)	δ_H (J in Hz)	δ_H (J in Hz)	δ_H (J in Hz)	δ_H (J in Hz)
2	4.43, m	4.42, m	4.37, m			
3	2.67, dd (16.8, 2.8)	2.67, dd (16.8, 3.0)	2.62, dd (16.8, 3.1)			
	2.74, m[d]	2.74, m[d]	2.72, m			
4						
5	7.81, d (7.8)	7.81, d (7.8)	7.78, d (7.5)	8.22, d (7.9)	8.22, d (7.9)	8.22, d (7.9)
6	7.02, t (7.9)	7.02, t (7.9)	6.98[d]	7.37, t (7.4)	7.37, t (7.5)	7.37, t (7.5)
7	7.54, t (8.7)	7.54, t (8.7)	7.49, d (7.3)	7.64, t (8.5)	7.64, t (7.7)	7.64, t (7.7)
8	7.05, d (8.5)	7.05, d (8.3)	7.00[e]	7.46, d (8.4)	7.44, d (8.4)	7.45, d (8.4)
9						
10						
1′						
2′	7.06, d (8.5)	6.81, d (1.8)	6.68[d]	6.73, br s	6.67, br s	6.75, br s
3′	6.70, d (8.5)					
4′			6.61, d (8.3)			6.71, dd (8.0, 1.6)
5′	6.70, d (8.5)	6.71, d (8.0)	7.06, t (7.7)	6.82, d (8.5)	6.82, d (8.0)	7.14, t (7.8)
6′	7.06, d (8.5)	6.67, dd (8.0, 1.9)	6.67[d]	6.75, br d (8.5)	6.70, br d (8.0)	6.77, br d (7.9)
7′	2.73, m[d]	2.74, m[d]	2.70, m[d]	3.02, t (7.5)	3.00, t (7.6)	3.02, t (7.7)
	2.81, m	2.82, m	2.79, m			
8′	1.96, m	1.98, m	1.93, m	3.14, t (7.5)	3.08, t (7.6)	3.11, t (7.7)
	2.13, m	2.14. m	2.10, m			
MeO-3					3.73, s	3.72, s
MeO-3′		3.81, s		3.80, s	3.77, s	

[a]Recorded in methanol-d_4 at 800 MHz. [b]Recorded in $CDCl_3$ at 400 MHz. [c]Recorded in $CDCl_3$ at 800 MHz. [d]Overlapped.

configuration of the dihydrokaempferol moiety in the structure of **5** was determined as 2*R*,3*R* based on the comparison of ECD data. Thus, compound **5** was defined as 2*R*,3*R*,7″*S*,8″*S* and the structure was assigned as shown.

Compound **6** (rhamnoneuronal C) was purified as a light yellow, amorphous powder with $[\alpha]_D^{25}$ −10 (*c* 0.1, MeOH). The molecular formula was determined as $C_{29}H_{20}O_9$ from the $[M - H]^-$ HRESIMS ion peak at *m/z* 511.1028 (calcd for $C_{29}H_{19}O_9$ 511.1035). The IR spectrum exhibited absorption bands for hydroxy (3336 cm^{-1}) and carbonyl (1611 cm^{-1}) functionalities. By comparing the 1D and 2D NMR data of **6** with those of **1**, compound **6** revealed a similar structure except for the double bond at C-7″ and C-8″. Two mutually coupled methines of **1** were replaced by the olefinic bond at C-7″ (δ_C 151.7) and C-8″ (δ_C 116.1) in compound **6**. This assignment was further confirmed by its HMBC correlations from H-2″/6″ at δ_H 7.45 (2H, d, *J* = 8.8 Hz) to C-7″ and from H-10″/14″ at δ_H 6.38 (2H, d, *J* = 2.2 Hz) to C-8″. The absolute configuration of compound **6** was determined to be 2*S*,3*S* compared to the ECD spectrum of **1**. Accordingly, compound **6** was assigned structurally as shown.

Compounds **1**−**6** have been proposed as a biosynthetic pathway for new flavonostilbenes produced by the fusion of resveratrol and dihydroflavonol in *R. balansae* (Scheme S1, Supporting Information). Peroxidase uses two resveratrol units to effectively oxidize and transfer electrons in phenols to produce resveratrol-derived radicals (I).[26] After the radical form (I) is transformed into the cationic form (II) through dismutase, the C−C bond was generated between resveratrol and dihydroflavonol units by nucleophilic attack from the resorcinol moiety in the A-ring of dihydroflavonol to the cation of resveratrol.[27] The highly reactive *p*-quinone methide is attacked by hydroxy at C-6 to form a dihydrobenzofuran ring through cyclization to produce compound **1**. Thus, the determined structure of compound **1** can be supported by the cationic form (II), which is the most stable structure. Finally, compound **1** can produce derivatives **3**−**5**, in which glucose is attached to the C-7 or C-4″ by *O*-glycosyl transferase, and compound **6** can be suggested to occur, as two methines in compound **1** are changed to olefins by dehydrogenase.

Compound **7** (balansechromanone A) was isolated as a pale yellow oil with $[\alpha]_D^{25}$ +83 (*c* 0.1, MeOH). A molecular formula of $C_{17}H_{16}O_3$ was established from the negative-ion HRESIMS data at *m/z* 267.1015 $[M - H]^-$ (calcd for $C_{17}H_{15}O_3$ 267.1021). The IR spectrum exhibited absorption bands for hydroxy (3361 cm^{-1}) and carbonyl (1607 cm^{-1}) groups. The ^{1}H NMR data (Table 1) displayed signals for 1,2-disubstituted benzene protons at δ_H 7.81 (1H, d, *J* = 7.8 Hz), 7.02 (1H, t, *J* = 7.9 Hz), 7.54 (1H, t, *J* = 8.7 Hz), and 7.05 (1H, d, *J* = 8.5 Hz), 1,4-disubstituted benzene protons at δ_H 7.06 (2H, d, *J* = 8.5 Hz) and 6.70 (2H, d, *J* = 8.5 Hz), two methylene protons at δ_H 2.81, 2.73, 2.13, and 1.96 (1H each, m), a set of mutually coupled oxymethine proton at δ_H 4.43 (1H, m), and methylene protons at δ_H 2.74 (1H, dd, *J* = 16.8, 2.8 Hz) and 2.67 (1H, m). The ^{13}C NMR data (Table 3) showed a total of 17 carbon resonances, including two oxygenated aromatic carbons at δ_C 156.7 and 163.3 and one carbonyl carbon at δ_C 194.7. The presence of a 2-(2-phenylethyl)-chromanone unit in compound **7** was determined based on the HMBC correlations from H-2 to C-8′ along with those from H_2-7′ to C-1′ and C-2′/6′ (Figure 1). The absolute configuration of compound **7** was assigned by means of an ECD comparative analysis using TDDFT at the def-SV(P)/B3LYP level (Figure 3D). The positive CE at 213 nm and the negative CE at 296 nm with the chromanone moiety suggested

https://dx.doi.org/10.1021/acs.jnatprod.0c00885
J. Nat. Prod. XXXX, XXX, XXX−XXX

Table 3. NMR Spectroscopic ^{13}C NMR Data for Compounds 1−12

	1[a]	2[b]	3[b]	4[b]	5[b]	6[b]		7[b]	8[b]	9[b]	10[c]	11[d]	12[d]
position	δ_C	δ_C	δ_C	δ_C	δ_C	δ_C	position	δ_C	δ_C	δ_C	δ_C	δ_C	δ_C
2	84.9	85.1	85.0	85.3	85.2	85.8	2	78.5	78.5	78.4	151.7	161.6	161.7
3	74.6	74.6	74.6	74.7	74.5	74.5	3	43.8	43.8	43.7	138.5	141.4	141.4
4	192.9	192.7	192.8	193.2	193.4	192.3	4	194.7	194.7	194.6	172.7	174.1	174.3
5	163.5	163.5	163.4	162.6	162.5	162.6	5	127.7	127.7	127.6	125.6	126.0	126.0
6	111.1	111.1	111.0	113.3	113.4	115.5	6	122.3	122.3	122.3	124.5	124.7	124.8
7	163.0	163.1	163.1	161.2	161.2	161.0	7	137.4	137.4	137.3	133.2	133.3	133.4
8	97.5	97.6	97.6	97.2	97.2	98.6	8	119.1	119.1	119.1	118.2	117.8	117.9
9	165.2	165.1	165.2	165.4	165.4	163.5	9	163.3	163.2	163.1	155.7	155.4	155.0
10	100.8	100.8	100.8	102.5	102.5	101.2	10	122.2	122.2	122.1	121.1	124.5	124.5
1′	129.5	130.1	129.5	129.3	129.2	129.5	1′	133.3	134.1	144.1	132.3	132.2	142.2
2′	130.4	115.9	130.3	130.4	130.5	130.4	2′	130.4	113.2	116.3	111.0	111.0	115.5
3′	116.1	146.3	116.1	116.1	116.1	116.1	3′	116.2	148.9	158.5	146.6	146.6	156.2
4′	159.1	147.1	159.2	159.2	159.3	159.2	4′	156.7	145.8	114.0	144.2	144.3	113.7
5′	116.1	116.1	116.1	116.1	116.1	116.1	5′	116.2	116.2	130.5	114.5	114.5	129.9
6′	130.4	120.9	130.3	130.4	130.5	130.4	6′	130.4	121.9	120.7	121.1	121.1	120.8
1″	133.3	133.5	136.6	132.9	133.1	123.2	7′	31.3	31.7	32.0	32.4	32.9	33.0
2″	128.2	128.2	127.8	128.2	128.1	129.1	8′	38.0	38.0	37.5	31.1	31.3	31.0
3″	116.4	116.4	117.9	116.4	116.4	116.2	MeO-3		56.3			60.7	60.7
4″	158.8	158.8	159.1	158.9	158.9	158.7	MeO-3′				56.0	55.9	
5″	116.4	116.4	117.9	116.4	116.4	116.2							
6″	128.2	128.2	127.8	128.2	128.1	129.1							
7″	96.9	96.9	96.3	97.0	96.9	151.7							
8″	55.1	55.1	55.3	55.4	55.2	116.1							
9″	146.2	146.2	146.2	146.3	146.5	136.1							
10″	106.7	106.8	106.8	106.7	106.7	109.7							
11″	159.8	159.8	159.9	160.1	160.2	159.3							
12″	102.1	102.2	102.2	102.5	102.5	102.9							
13″	159.8	159.8	159.9	160.1	160.2	159.3							
14″	106.7	106.8	106.8	106.7	106.7	109.7							
Glc													
1‴			102.2	101.4	101.3								
2‴			74.9	74.7	74.7								
3‴			78.0	77.2	77.4								
4‴			71.4	70.9	70.9								
5‴			78.2	78.3	78.3								
6‴			62.5	62.2	62.2								

[a]Recorded in methanol-d_4 and at 100 MHz. [b]Recorded in methanol-d_4 and at 200 MHz. [c]Recorded in $CDCl_3$ and at 100 MHz. [d]Recorded in $CDCl_3$ at 200 MHz.

that the absolute configuration at C-2 is 2*R*. Therefore, compound **7** was assigned as shown.

Compound **8** (balansechromanone B) was obtained as a pale yellow oil with $[\alpha]_D^{25}$ +101 (*c* 0.1, MeOH). The molecular formula was determined as $C_{18}H_{18}O_4$ from the positive HRESIMS ion at *m/z* 299.1281 $[M + H]^+$ (calcd for $C_{18}H_{19}O_4$ 299.1283). The IR spectrum exhibited absorption signals for hydroxy (3426 cm^{-1}) and carbonyl (1606 cm^{-1}) functionalities. Its NMR data indicated that compound **8** is structurally similar to **7** except for the benzene system at the phenylethyl moiety. The A_2B_2 system of the 2-phenylethyl in **7** was changed to an ABX system at δ_H 6.81 (1H, d, *J* = 1.8 Hz), 6.71 (1H, d, *J* = 8.0 Hz), and 6.67 (1H, dd, *J* = 8.0, 1.9 Hz). In addition, compound **8** showed the presence of a methoxy resonance at δ_H 3.81 (3H, s; δ_C 56.3). The position of the methoxy group was located at C-3′ based on the HMBC cross-peaks from the methoxy group to C-3′ (δ_C 148.9) and the NOESY correlation between the methoxy group and H-2′ (δ_H 6.73). A comparison of the experimental ECD spectra of compound **7** with those of **8** indicated that the absolute configuration of **8** is 2*R* (Figure 3D). Thus, compound **8** was assigned as shown.

Compound **9** (balansechromanone C) was obtained as a pale yellow oil with $[\alpha]_D^{25}$ +85 (*c* 0.1, MeOH). The molecular formula was determined as $C_{17}H_{16}O_3$ from the negative HRESIMS ion at *m/z* 267.1012 $[M - H]^-$ (calcd for $C_{17}H_{15}O_3$ 267.1021). The IR spectrum exhibited absorption bands for hydroxy (3362 cm^{-1}) and carbonyl (1605 cm^{-1}) groups. The 1D and 2D NMR data were similar to **7** except for the 1,3-disubstituted benzene group in compound **9**. Its HMBC correlations from H_2-7′ at δ_H 2.79 and 2.70 to C-1′ (δ_C 144.1), C-2′ (δ_C 116.3), and C-6′ (δ_C 121.9) supported these inferences. The absolute configuration of C-2 was determined as the same as compound **7** based on its ECD spectrum (Figure 3D). Thus, compound **9** was assigned as shown.

Compound **10** (balansechromone A) was isolated as a pale yellow oil with $[\alpha]_D^{25}$ +60 (*c* 0.1, MeOH). The molecular formula of this compound was determined as $C_{18}H_{16}O_5$ from

https://dx.doi.org/10.1021/acs.jnatprod.0c00885
J. Nat. Prod. XXXX, XXX, XXX−XXX

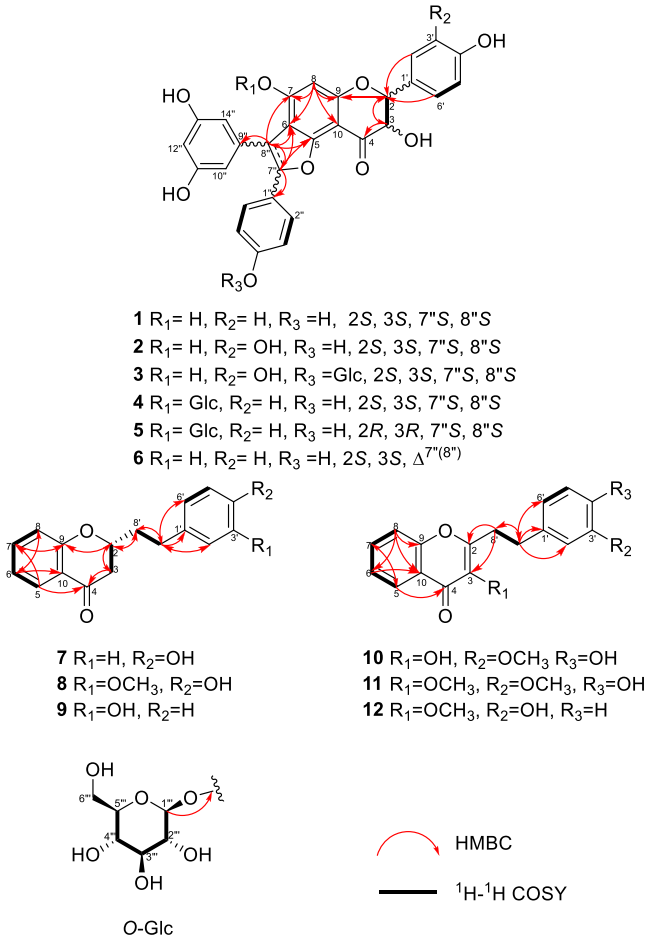

Figure 1. Key HMBC (red arrows) and ^{1}H−^{1}H COSY (bold black lines) correlations of compounds **1**−**12**.

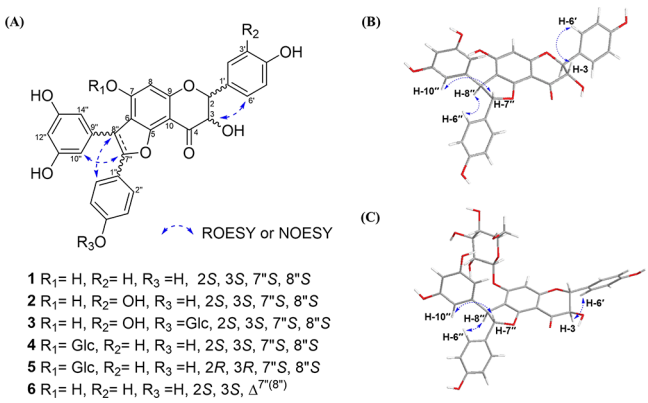

Figure 2. Key ROESY/NOESY correlations of compounds **1**−**5** (A). 3D model of the lowest energy conformation of compounds **1** (B) and **5** (C).

the negative HRESIMS ion at m/z 311.0913 [M − H]$^-$ (calcd for $C_{18}H_{15}O_5$ 311.0919). The IR absorption bands showed the presence of hydroxy (3279 cm^{-1}) and carbonyl (1610 cm^{-1}) groups. Its ^{1}H NMR data (Table 2) exhibited signals for 1,2-disubstituted benzene protons at δ_H 8.22 (1H, d, J = 7.9 Hz), 7.64 (1H, t, J = 8.5 Hz), 7.46 (1H, d, J = 8.4 Hz), and 7.37 (1H, t, J = 7.4 Hz), 1,3,4-trisubstituted benzene protons at δ_H 6.82 (1H, d, J = 8.5 Hz), 6.75 (1H, br d, J = 8.5 Hz), and 6.73 (1H, br s), two mutually coupled methylene protons at δ_H 3.14 (2H, t, J = 7.5 Hz) and 3.02 (2H, t, J = 7.5 Hz), and a methoxy group at δ_H 3.80 (3H, s). The ^{13}C NMR spectrum (Table 3) of **10** showed a set of olefinic carbons at δ_C 151.7 and 138.5 and a conjugated carbonyl carbon at δ_C 172.7. The presence of the methoxy group at C-3 was deduced by the HMBC correlation from MeO-3′ at δ_H 3.80 to C-3′ (δ_C 146.6) and the NOESY correlation between MeO-3′ and H-2′ (δ_H 6.73). The comparison of the 1D and 2D NMR data of compound **10** with those of **8** suggested that H-2 (δ_C 78.5) and H_2-3 (δ_C 43.8) in compound **8** were replaced by a 2,3-olefinic bond at δ_C 151.7 and 138.5 in **9**. Its HMBC correlations from H_2-8′ to C-2 and C-3 confirmed that compound **9** has a 3-hydroxychromone moiety (Figure 1). Thus, compound **10** was determined to be a 3-hydroxy-2-(2-phenylethyl)chromone derivative as shown.

Compound **11** (balansechromone B) was isolated as a light yellowish oil with $[\alpha]_D^{25}$ +64 (c 0.1, MeOH). Its molecular formula was determined as $C_{19}H_{18}O_5$ from the [M + H]$^+$ HRESIMS ion at m/z 327.1232 (calcd for $C_{19}H_{19}O_5$ 327.1232). The IR spectrum exhibited absorption signals for hydroxy (3362 cm^{-1}) and carbonyl (1618 cm^{-1}) functionalities. A comparative analysis of the NMR spectra of compounds **10** and **11** showed the presence of an additional methoxy group at δ_H 3.73 (3H, s; δ_C 60.7) in **11**. The position of the additional methoxy group was suggested by the HMBC correlation between MeO (δ_H 3.73) and C-3 (δ_C 141.4). These structural changes were confirmed by the downfield shift of C-2 and C-3 from δ_C 151.7 and 138.5 of **10** to δ_C 161.6 and 141.4 of compound **11**. Finally, compound **11** was assigned as shown.

Compound **12** (balansechromone C) was isolated as a light yellowish oil with $[\alpha]_D^{25}$ +63 (c 0.1, MeOH). The molecular formula of **12** was determined to be $C_{18}H_{16}O_4$ from its [M − H]$^-$ HRESIMS ion peak at m/z 295.0977 (calcd for $C_{18}H_{15}O_4$ 295.0970). The IR spectrum exhibited the absorption signals of hydroxy (3331 cm^{-1}) and carbonyl (1617 cm^{-1}) functionalities. On comparing the NMR spectra of compound **12** with those of **11**, the structure of **12** was similar to **11** except for the signals for the benzene ring of the 2-phenylethyl moiety. The 1,3,4-trisubstituted benzene moiety in **11** was replaced by a 1,3-disubstituted benzene group in **12**, and this assignment was deduced by the proton and carbon signals at δ_H 7.14 (1H, t, J = 7.8 Hz; δ_C 129.9), 6.77 (1H, br d, J = 7.9 Hz; δ_C 120.8), 6.75 (1H, br s; δ_C 115.5), and 6.71 (1H, dd, J = 8.0, 1.6 Hz; δ_C 113.7). These results were confirmed through the HMBC correlations from H_2-7′ (δ_H 3.02) to C-1 (δ_C 142.2), C-2 (δ_C 115.5), and C-6 (δ_C 120.8).[28] Therefore, compound **11** was assigned as shown.

Based on the NMR data and optical rotations as well as literature values, four known compounds were elucidated as (2*R*,4a*S*,7*R*,8a*R*)-7-(3-hydroxyprop-1-en-2-yl)-4a-methyl-1-methylenedecahydronaphthalen-2-ol (**13**),[29] viscic acid (**14**),[30] (+)-hinokinin (**15**),[31] and (2*R*,3*S*)-2-hydroxy-2,3-bis(4-hydroxy-3-methoxybenzyl)-4-butanolide (**16**).[32]

To explore the senolytic activity of the new isolated compounds, the ability to selectively kill senescent cells was evaluated by exposing the compounds to proliferating cells and senescent human dermal fibroblast (HDF) cells and comparing the results. The 12 new compounds isolated from *R. balansae*, at a 20 μM concentration, were used to treat proliferating cells, and toxicity was not observed (Figure 4A). Based on this, cell viability was evaluated by treating senescent cells with the isolated compounds at the same concentration. Among these

https://dx.doi.org/10.1021/acs.jnatprod.0c00885
J. Nat. Prod. XXXX, XXX, XXX−XXX

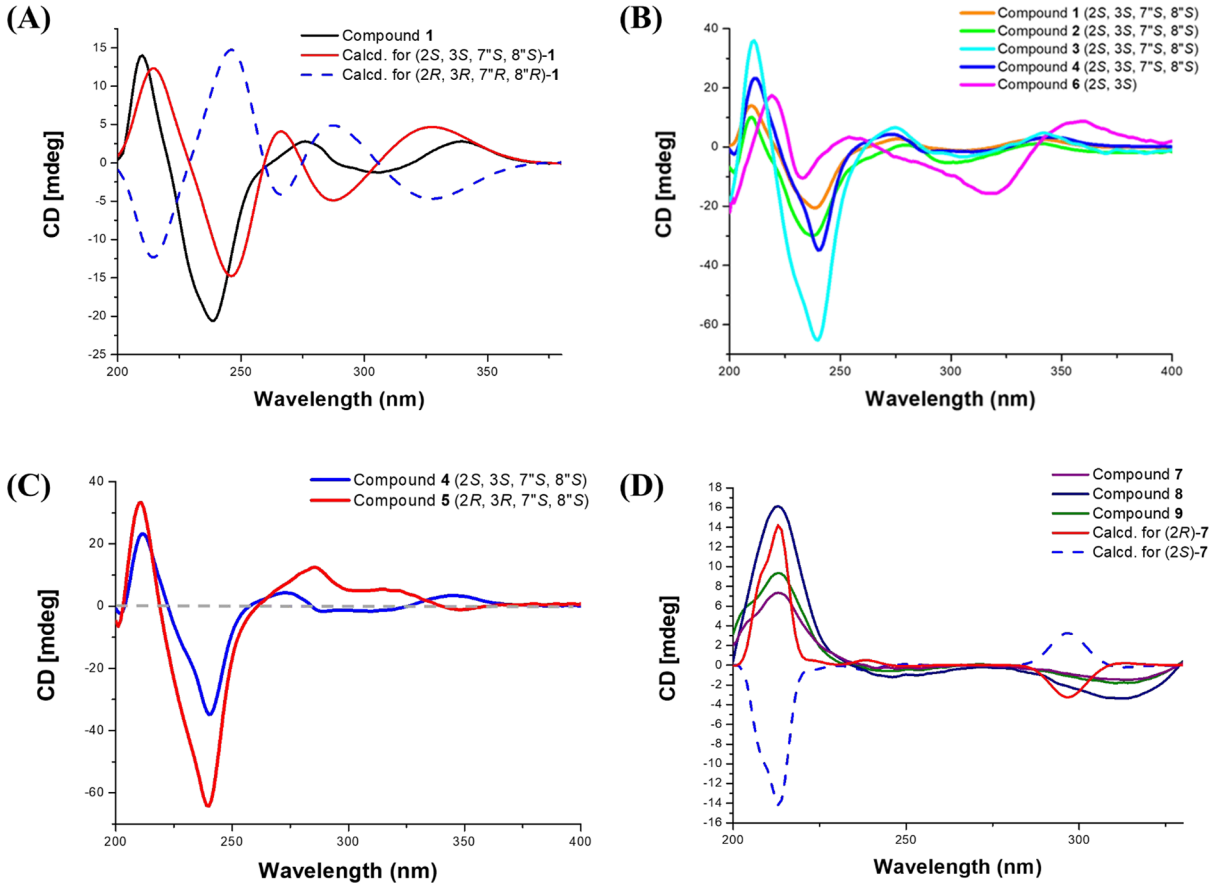

Figure 3. Comparative analysis of the experimental and computational ECD spectra (shift = 16 nm; σ = 0.30) of compounds **1**−**4** and **6** (A and B) and the assignment of the absolute configuration of **5** (2*R*,3*R*,7″*S*,8″*S*) by comparing the spectra to that of compound **4** (2*S*,3*S*,7″*S*,8″*S*) (C). Comparison of the experimental and computational ECD spectra (shift: 0 nm; σ = 0.1) of compounds **7**−**9** (D).

compounds, rhamnoneuronal C (**6**) and balansechromanones A (**7**) and B (**8**) showed the greatest potential in regard to senolytic activity. In particular, the cell viability of the rhamnoneuronal C (**6**)-treated group was reduced by 34% in the senescent cells compared with the cell viability of the control, thereby showing the most specific senolytic property (Figure 4B). Additionally, a luciferase reporter assay system was utilized with the newly isolated compounds to evaluate their ability to inhibit the promoter activity of p16INK4A, which is a specific marker in senescent cells. After treatment with the compounds, rhamnoneuronal C (**6**) significantly reduced the promoter activity of p16INK4A by 32%. Thus, rhamnoneuronal C (**6**) may be expected to possess p16INK4A-dependent senolytic activity (Figure 4C).

In conclusion, the present study proposes new senolytic candidates that selectively remove senescent cells to reduce their harmful effects on normal replicating HDF cells. In the cell viability comparison experiment between young and aged cells to determine the senolytic properties of the isolates, compounds **6**−**8** were shown to have potential for use as lead compounds of senolytic agents. Furthermore, the transcriptional activation of the p16INK4A promoter, a representative senescence marker, was reduced markedly only with compound **6**, whereas compounds **7** and **8** do not show this reduction. From these observations, it is likely that compounds **6** and **7** (or compound **8**) exert senolytic properties via different modes of action. Since a direct link based on convincing evidence between cell death and the inhibition of p16INK4A has not been fully established until now, further studies on the relationship between p16INK4A and cell death will be needed. Taken together, compounds **6**−**8** may have use as new senolytic agent leads and hence contribute to relevant mechanistic studies.

■ EXPERIMENTAL SECTION

General Experimental Procedures. Optical rotations were acquired with a JASCO P-2000 polarimeter (JASCO, Tokyo, Japan). UV and ECD spectra were obtained using a Chirascan-Plus CD spectrometer (Applied Photophysics, Leatherhead, UK). IR spectra were recorded using a JASCO FT/IR-4200 spectrometer. NMR data were measured using a JNM-ECZ-400S (JEOL, Tokyo, Japan) and Bruker Avance-800 MHz spectrometer (Bruker, Billerica, MA, USA). HRESIMS were acquired with an Agilent 6530 Q-TOF mass spectrometer (Agilent Technologies, Santa Clara, CA, USA) and a Waters Xevo G2 QTOF mass spectrometer (Waters, Milford, MA, USA). Zeoprep silica gel (63−200 μm, Zeochem, uetikon am See, Switzerland), Cosmosil 75C_{18}-OPN (75 μm, Nacalai Tesque, Kyoto, Japan), and Sephadex LH-20 (Sigma-Aldrich, St. Louis, MO, USA) were used for column chromatography. Thin-layer chromatography (TLC) analyses were performed with TLC silica gel 60 F_{254} and TLC silica gel 60 RP-18 F_{254S} plates (Merck, Darmstadt, Germany). Preparative HPLC was carried out using a Gilson system (Gilson, Villiers-le-Bel, France) with a UV detector at 205 or 254 nm and an Optima Pak C_{18} column (10 × 250 mm, 10 μm, RS Tech, Seoul, Korea).

Plant Material. The plant material was collected from the Ha Vi commune, Bach Thong district, Bac Kan province, Vietnam (22°13′08.3″ N, 105°50′05.4″ E), in April 2018. Based on morphological characteristics, the samples were identified as

https://dx.doi.org/10.1021/acs.jnatprod.0c00885
J. Nat. Prod. XXXX, XXX, XXX−XXX

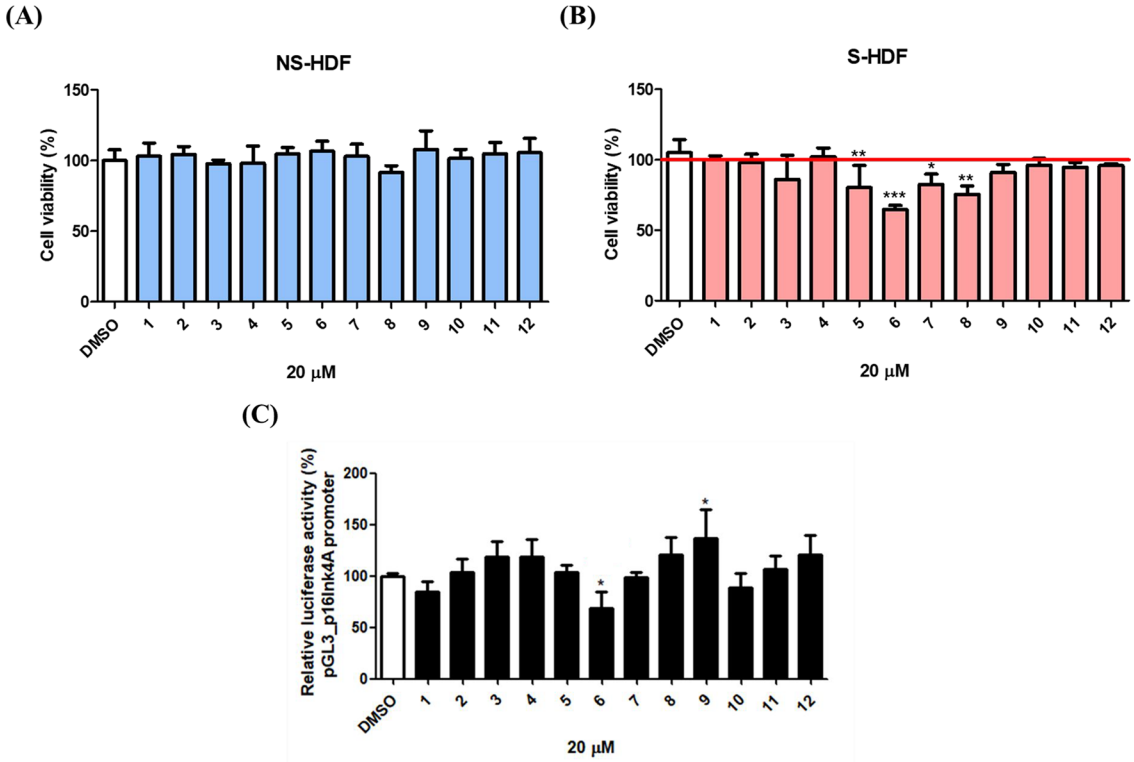

Figure 4. Compounds **6**−**8** selectively removed targeted senescent cells. Proliferating (A) or senescent human dermal fibroblast cells (B) were exposed to 20 μM of the various isolated compounds for 3 days. The cell viability percentages were evaluated using the MTT method. The effect of 12 different compounds on the promoter activity of p16INK4A in human dermal fibroblasts (C). Compounds **1**−**12** were exposed to cells for 24 h, and the activity of the p16INK4A promoter was shown by comparing the compound-treated groups to the untreated group.

Rhamnoneuron balansae (Drake) Gilg by Professor Duc Trong Nghiem, Department of Botany, Hanoi University of Pharmacy, Hanoi, Vietnam. A voucher specimen was deposited in the Medicinal Herbarium of Hanoi University of Pharmacy (HNIP) with the accession number HNIP.18510/15.

Extraction and Isolation. The roots of *R. balansae* (30 kg) were extracted with 70% EtOH (3 × 10 L), and the resulting extract was freeze-dried to yield a brown powder (730 g). This extract was suspended in water and sequentially partitioned with *n*-BuOH (3 × 4 L). The *n*-BuOH-soluble part (220 g) was preadsorbed on silica gel for column chromatography and eluted with an *n*-hexane and EtOAc gradient (2:1 → 0:1, v/v) to yield four fractions (R1−R4). Fraction R2 (10 g) was separated into 10 fractions (R2.1−R2.10) via RP-C_{18} column chromatography and eluted with a MeOH/H_2O gradient (3:7 → 1:0, v/v). Fraction R2.6 (1.0 g) was subjected to Sephadex LH-20 column chromatography (CC) and eluted with MeOH to afford six subfractions (R2.6.1−R2.6.6). Fraction R2.6.3 was purified by preparative HPLC with CH_3CN/H_2O (3:7, 2 mL/min) to afford compounds **10** (15.1 mg), **11** (8.2 mg), and **12** (10.5 mg). Fraction R2.8 (1.2 g) was separated by Sephadex LH-20 CC and eluted with MeOH to obtain seven subfractions (R2.8.1−R2.8.7). Fraction R2.8.2 (200 mg) was purified by HPLC and eluted with CH_3CN/H_2O (4:6, 2 mL/min) to obtain compounds **13** (10 mg) and **14** (5.0 mg). Fraction R2.8.4 was purified by preparative HPLC with MeOH/H_2O (7:3, 2 mL/min) to afford compounds **7** (1.7 mg), **8**, (3.0 mg), and **9** (3.0 mg). Fraction R2.8.5 (70 mg) was purified by HPLC and eluted with MeOH/H_2O (6:4, 2 mL/min) to obtain compound **15** (5.7 mg). Fraction R4 (120 g) was separated into 19 fractions (R4.1−R4.19) via RP-C_{18} CC and eluted with a MeOH/H_2O gradient (2:8 → 1:0, v/v). Fraction R4.8 was separated by Sephadex LH-20 CC and eluted with MeOH to afford four subfractions (R4.8.1−R4.8.4). Fraction R4.8.3 (50 mg) was purified by HPLC and eluted with MeOH/H_2O (3:7, 2 mL/min) to obtain compounds **3** (3.0 mg), **4** (3.1 mg), and **5** (2.0 mg). Fraction R4.10 was separated by Sephadex LH-20 CC and eluted with MeOH to afford six subfractions (R4.10.1−R4.10.6). Fraction R4.10.6 (70 mg) was purified by HPLC and eluted with MeOH/H_2O (3:7, 2 mL/min) to obtain compounds **2** (2.1 mg) and **6** (2.0 mg). Fraction R4.12 was separated by Sephadex LH-20 CC and eluted with MeOH to afford five subfractions (R4.12.1−R4.12.5). Fraction R4.12.3 (35 mg) was purified by HPLC and eluted with MeOH/H_2O (4:6, 2 mL/min) to obtain compound **1** (5.0 mg).

*Rhamnoneuronal A (**1**):* yellowish powder; $[\alpha]_D^{20}$ −15 (*c* 1.0, MeOH); UV (MeOH) λ_{max} (log ε) 195 (3.96), 225 (3.82), 285 (3.21) nm; IR ν_{max} 3375, 2947, 2835, 1659, 1618, 1450, 1415, 1114, 1026, 693 cm^{-1}; ^1H and ^{13}C NMR data, see Tables 1 and 3; HRESIMS *m/z* 513.1192 $[M - H]^-$ (calcd for $C_{29}H_{21}O_9$, 513.1191).

*Rhamnoneuronal B (**2**):* yellowish powder; $[\alpha]_D^{20}$ −52 (*c* 1.0, MeOH); UV (MeOH) λ_{max} (log ε) 200 (3.91), 225 (3.71), 285 (3.12) nm; IR ν_{max} 3357, 1612, 1517, 1454, 1255, 1073, 1019 cm^{-1}; ^1H and ^{13}C NMR data, see Tables 1 and 3; HRESIMS *m/z* 529.1117 $[M - H]^-$ (calcd for $C_{29}H_{21}O_{10}$, 529.1140).

*Rhamnoneuroside A (**3**):* yellowish powder; $[\alpha]_D^{20}$ −98 (*c* 1.0, MeOH); UV (MeOH) λ_{max} (log ε) 195 (3.96), 225 (3.67), 285 (3.08) nm; IR ν_{max} 3389, 1600, 1358, 1055, 1012, 835, 671 cm^{-1}; ^1H and ^{13}C NMR data, see Tables 1 and 3; HRESIMS *m/z* 675.1716 $[M - H]^-$ (calcd for $C_{35}H_{31}O_{14}$, 675.1714).

*Rhamnoneuroside B (**4**):* yellowish powder; $[\alpha]_D^{20}$ −140 (*c* 1.0, MeOH); UV (MeOH) λ_{max} (log ε) 195 (3.96), 225 (3.67), 285 (3.08) nm; IR ν_{max} 3347, 1616, 1085, 1028, 835, 687 cm^{-1}; ^1H and ^{13}C NMR data, see Tables 1 and 3; HRESIMS *m/z* 675.1724 $[M - H]^-$ (calcd for $C_{35}H_{31}O_{14}$, 675.1719).

*Rhamnoneuroside C (**5**):* yellowish powder; $[\alpha]_D^{20}$ −45 (*c* 1.0, MeOH); UV (MeOH) λ_{max} (log ε) 195 (3.95), 230 (3.65), 285 (3.09) nm; IR ν_{max} 3361, 1617, 1079, 982, 836, 685 cm^{-1}; ^1H and ^{13}C NMR data, see Tables 1 and 3; HRESIMS *m/z* 675.1716 $[M - H]^-$ (calcd for $C_{35}H_{31}O_{14}$, 675.1714).

*Rhamnoneuronal C (**6**):* yellowish powder; $[\alpha]_D^{20}$ −10 (*c* 1.0, MeOH); UV (MeOH) λ_{max} (log ε) 195 (3.94), 225 (3.84), 300 (3.48) nm; IR ν_{max} 3336, 1611, 1517, 1054, 1032, 671 cm^{-1}; ^1H and

https://dx.doi.org/10.1021/acs.jnatprod.0c00885
J. Nat. Prod. XXXX, XXX, XXX−XXX

^{13}C NMR data, see Tables 1 and 3; HRESIMS m/z 511.1028 [M − H]$^-$ (calcd for $C_{29}H_{19}O_9$, 511.1035).

Balansechromanone A (7): yellowish powder; $[\alpha]_D^{20}$ +83 (c 1.0, MeOH); UV (MeOH) λ_{max} (log ε) 195 (4.51), 215 (4.29), 250 (3.71) nm; IR ν_{max} 3361, 1607, 1465, 1226, 831, 764, 662 cm^{-1}; ^{1}H and ^{13}C NMR data, see Tables 2 and 3; HRESIMS m/z 267.1015 [M − H]$^-$ (calcd for $C_{17}H_{15}O_3$, 267.1021).

Balansechromanone B (8): yellowish powder; $[\alpha]_D^{20}$ +101 (c 1.0, MeOH); UV (MeOH) λ_{max} (log ε) 195 (4.51), 215 (4.29), 250 (3.71) nm; IR ν_{max} 3426, 1687, 1606, 1514, 1463, 1228, 1150, 1032, 882, 765, 632 cm^{-1}; ^{1}H and ^{13}C NMR data, see Tables 2 and 3; HRESIMS m/z 299.1281 [M − H]$^+$ (calcd for $C_{18}H_{19}O_4$, 299.1283).

Balansechromanone C (9): yellowish powder; $[\alpha]_D^{20}$ +85 (c 1.0, MeOH); UV (MeOH) λ_{max} (log ε) 200 (4.62), 220 (4.63), 250 (3.23) nm; IR ν_{max} 3362, 1671, 1605, 1464, 1314, 1150, 882, 615 cm^{-1}; ^{1}H and ^{13}C NMR data, see Tables 2 and 3; HRESIMS m/z 267.1012 [M − H]$^-$ (calcd for $C_{17}H_{15}O_3$, 267.1021).

Balansechromone A (10): yellowish powder; $[\alpha]_D^{20}$ +60 (c 1.0, MeOH); UV (MeOH) λ_{max} (log ε) 200 (4.56), 235 (4.54), 283 (4.04), 320 (3.80) nm; IR ν_{max} 3279, 1610, 1515, 1215, 811, 616 cm^{-1}; ^{1}H and ^{13}C NMR data, see Tables 2 and 3; HRESIMS m/z 311.0913 [M − H]$^-$ (calcd for $C_{18}H_{15}O_5$, 311.0919).

Balansechromone B (11): yellowish powder; $[\alpha]_D^{20}$ +64 (c 1.0, MeOH); UV (MeOH) λ_{max} (log ε) 200 (4.43), 235 (4.47), 283 (4.03), 320 (3.90) nm; IR ν_{max} 3362, 1618, 1515, 1211, 1032, 630 cm^{-1}; ^{1}H and ^{13}C NMR data, see Tables 2 and 3; HRESIMS m/z 327.1232 [M + H]$^+$ (calcd for $C_{18}H_{19}O_5$, 327.1232).

Balansechromone C (12): yellowish powder; $[\alpha]_D^{20}$ +63 (c 1.0, MeOH); UV (MeOH) λ_{max} (log ε) 200 (4.54), 235 (4.40), 283 (4.01), 320 (3.82) nm; IR ν_{max} 3331, 1617, 1467, 1232, 759, 700 cm^{-1}; ^{1}H and ^{13}C NMR data, see Tables 2 and 3; HRESIMS m/z 295.0977 [M − H]$^-$ (calcd for $C_{18}H_{15}O_4$, 295.0970).

Sugar Analysis. The absolute configurations of the monosaccharide units present in the isolated compounds were analyzed with the same procedures as in a previous investigation.[33] Detailed information is shown in the Supporting Information (Figure S100).

Preparation of the (*S*)-MTPA and (*R*)-MTPA Ester Derivatives of Compound 1. Compound **1** (1.0 mg, 1.95 μmol) was dissolved in dry pyridine (489.3 μL, 6.05 μmol, 3.1 equiv), and then anhydrous $CHCl_3$ was added to the residue. *S*-(+)-MTPA-Cl (0.73 μL, 3.9 μmol, 2.0 equiv) and 4-dimethylaminopyridine (0.3 mg) were added to the mixture and stirred at room temperature for 3 h. The reaction solution was checked by TLC analysis and fractionated three times with ethyl acetate and water. The ethyl acetate extract was dried using an evaporator, and the ^{1}H NMR data were directly recorded due to the small scale of the reaction. The above step was repeated using *R*-(−)-MTPA-Cl to give the ^{1}H NMR spectrum of the (*S*)-MTPA ester derivative. The use of the Mosher method was based on a previous paper.[24]

Computational ECD Analysis. The computational analysis of compounds **1** and **7** was performed using MMFF94 calculations with a search limit of 1.0 kcal/mol in Conflex 7 (ConflexCorp., Tokyo, Japan). We used TmoleX 4.4 and Turbomole to optimize the ground-state geometry of the main conformers using the def-SV (P) basis set and the B3LYP functional levels with compounds **1** and **7**. The computed ECD spectra of all optimized conformers were represented by TDDFT using the 6-31G basis set and the B3LYP functional levels for compound **1** and the def-SV(P) basis set and the B3LYP functional levels for compound **7** through Boltzmann distributions. The detailed calculation method was performed using the same process as reported in a previous paper.[33] All calculated ECD spectra were generated with a UV shift of 16 nm and σ = 0.3 eV for compound **1** and without a UV shift and σ = 0.1 for **7** using Specdis 1.70.1 (University of Würzburg, Würzburg, Germany).

Cell Culture. A primary culture of human dermal fibroblast cells was kindly provided by Professor Kyung A. Cho of Chonnam National University. HDF cells were maintained under subconfluent conditions in Dulbecco's modified Eagle's medium (DMEM, HyClone, Logan, UT, USA) supplemented with 10% fetal bovine serum (FBS, HyClone) and 1% penicillin/streptomycin (P/S, HyClone) in an atmosphere of 5% CO_2 and incubated at 37 °C. Cellular senescence was induced by the replication of passages. After the cells were cultured to passage 35, the cellular senescence level was confirmed by monitoring the colorimetric analysis of the senescence-associated β-galactosidase and mRNA expression level of p16INK4A (Figure S103, Supporting Information).

Cell Viability Assay. The cytotoxicity of compounds was evaluated using an MTT (3-(4,5-dimethylthiazol-2-yl)-2,5-diphenyltetrazolium bromide) assay (Sigma, MO, USA). HDF cells were seeded at a density of 5×10^3 cells/well in 96-well plates and incubated for 24 h to attach cells before being treated with the isolated compounds. Then, the cells were treated with the test compounds at a concentration of 20 μM and incubated for 3 days. To avoid the solvent toxicity of dimethyl sulfoxide (DMSO) in the medium, the final DMSO concentration was kept at 0.05%. Then, 20 μL of a 2 mg/mL MTT solution was added to each well, followed by incubation for 2 h. To measure the absorbance, a Versamax microplate reader (VersaMax, PA, USA) was used at 570 nm.[16]

Luciferase Reporter Assay. Reporter gene transfection was performed using Lipofectamine LTX (Thermo Fisher Scientific) in HDF cells. Prior to the experiment, transfection efficiency was measured using a GFP-tagged plasmid. Subsequently, HDF cells were cultured at a density of 3×10^4 cells/well in 24-well plates. After 24 h, the medium was transferred to fresh DMEM supplemented only with 10% FBS. The pGL3_p16INK4A promoter (0.4 μg), which encodes firefly luciferase driven by the p16INK4A promoter and β-galactosidase (0.1 μg, encoding Renilla luciferase in 25 μL of Opti-MEM), was incubated with Lipofectamine LTX (0.75 μL, Invitrogen, Carlsbad, CA, USA) and PLUS reagent (0.25 μL, Invitrogen) in 25 μL of Opti-MEM (Gibco/Thermo Fisher Scientific, Waltham, MA, USA) for 10 min at room temperature. Then, 50 μL of the DNA−lipid complex was added to each well. The mixture was exposed to the cells for 5 h and incubated overnight with DMEM supplemented with 10% FBS. Next, the cells were treated with DMSO or the isolated components in a serum-free medium for an additional 24 h. The luciferase activity was determined as the percentage of firefly/Renilla luciferase activity. The activity of the p16INK4A promoter in the presence of compounds relative to that of the vehicle is shown.[16]

Statistical Analysis. Data are expressed as the means ± standard deviations (SDs) of three independent experiments and were calculated and plotted by one-way analysis of variance (ANOVA). Statistically significant differences are indicated as the following: $^*p < 0.05$, $^{**}p < 0.01$, and $^{***}p < 0.001$.

■ ASSOCIATED CONTENT

Supporting Information

The Supporting Information is available free of charge at https://pubs.acs.org/doi/10.1021/acs.jnatprod.0c00885.

NMR, HRESIMS, and IR spectra of compounds **1**−**12**; ^{1}H NMR spectra of the *R*- and *S*-MTPA esters of **1**; 3D structures of the *R*- and *S*-MTPA esters; and detailed in silico predicted ECD data of compounds **1** and **7** (PDF)

■ AUTHOR INFORMATION

Corresponding Author

Won-Keun Oh − *Korea Bioactive Natural Material Bank, Research Institute of Pharmaceutical Sciences, College of Pharmacy, Seoul National University, Seoul 08826, Republic of Korea;* orcid.org/0000-0003-0761-3064; Phone: +82-2-880-7872; Email: wkoh1@snu.ac.kr

Authors

Hyo-Moon Cho − *Korea Bioactive Natural Material Bank, Research Institute of Pharmaceutical Sciences, College of Pharmacy, Seoul National University, Seoul 08826, Republic of Korea;* orcid.org/0000-0003-3447-8726

https://dx.doi.org/10.1021/acs.jnatprod.0c00885
J. Nat. Prod. XXXX, XXX, XXX−XXX

Yae-Rin Lee − *Korea Bioactive Natural Material Bank, Research Institute of Pharmaceutical Sciences, College of Pharmacy, Seoul National University, Seoul 08826, Republic of Korea*

Ba-Wool Lee − *Korea Bioactive Natural Material Bank, Research Institute of Pharmaceutical Sciences, College of Pharmacy, Seoul National University, Seoul 08826, Republic of Korea;* orcid.org/0000-0002-4944-5145

Mi Zhang − *Korea Bioactive Natural Material Bank, Research Institute of Pharmaceutical Sciences, College of Pharmacy, Seoul National University, Seoul 08826, Republic of Korea*

Byeol Ryu − *Korea Bioactive Natural Material Bank, Research Institute of Pharmaceutical Sciences, College of Pharmacy, Seoul National University, Seoul 08826, Republic of Korea;* orcid.org/0000-0002-3405-2875

Du-Trong Nghiem − *Department of Botany, Hanoi University of Pharmacy, Hanoi, Vietnam*

Ha-Thanh-Tung Pham − *Department of Botany, Hanoi University of Pharmacy, Hanoi, Vietnam*

Complete contact information is available at: https://pubs.acs.org/10.1021/acs.jnatprod.0c00885

Notes

The authors declare no competing financial interest.

■ ACKNOWLEDGMENTS

This research was funded by grants from the Korea Bioactive Natural Material Bank (NRF-2017M3A9B8069409) and from the Basic Science Research Program (NRF-2017R1E1A1-A01074674) through the National Research Foundation of Korea funded by the Ministry of Science, ICT and Planning. We thank Dr. Hoang Minh Chau, CEO of the Nam Duoc Pharmaceutical Joint Stock Company in Vietnam, for 70% EtOH extraction and freeze-drying of *R. balansae* roots.

■ REFERENCES

(1) Woolf, S. H.; Schoomaker, H. *JAMA* **2019**, *322*, 1996−2016.
(2) Luo, J.; Mills, K.; le Cessie, S.; Noordam, R.; Van Heemst, D. *Ageing Res. Rev.* **2020**, *57*, 100982.
(3) Wissler Gerdes, E. O.; Zhu, Y.; Tchkonia, T.; Kirkland, J. L. *FEBS J.* **2020**, *287*, 2418−2427.
(4) Kirkland, J. L.; Tchkonia, T. *EBioMedicine* **2017**, *21*, 21−28.
(5) Myrianthopoulos, V.; Evangelou, K.; Vasileiou, P. V.; Cooks, T.; Vassilakopoulos, T. P.; Pangalis, G. A.; Kouloukoussa, M.; Kittas, C.; Georgakilas, A. G.; Gorgoulis, V. G. *Pharmacol. Ther.* **2019**, *193*, 31−49.
(6) Hickson, L. J.; Prata, L. G. L.; Bobart, S. A.; Evans, T. K.; Giorgadze, N.; Hashmi, S. K.; Herrmann, S. M.; Jensen, M. D.; Jia, Q.; Jordan, K. L.; Kellogg, T. A.; Khosla, S.; Koerber, D. M.; Lagnado, A. B.; Lawson, D. K.; LeBrasseur, N. K.; Lerman, L. O.; McDonald, K. M.; McKenzie, T. J.; Passos, J. F.; Pignolo, R. J.; Pirtskhalava, T.; Saadiq, I. M.; Schaefer, K. K.; Textor, S. C.; Victorelli, S. G.; Volkman, T. L.; Xue, A.; Wentworth, M. A.; Gerdes, E. O. W.; Zhu, Y.; Tchkonia, T.; Kirkland, J. L. *EBioMedicine* **2019**, *47*, 446−456.
(7) Soto-Gamez, A.; Demaria, M. *Drug Discovery Today* **2017**, *22*, 786−795.
(8) Childs, B. G.; Baker, D. J.; Wijshake, T.; Conover, C. A.; Campisi, J.; Van Deursen, J. M. *Science* **2016**, *354*, 472−477.
(9) Gorgoulis, V. G.; Pefani, D. E.; Pateras, I. S.; Trougakos, I. P. *J. Pathol.* **2018**, *246*, 12−40.
(10) He, S.; Sharpless, N. E. *Cell* **2017**, *169*, 1000−1011.
(11) Li, J.; Rix, U.; Fang, B.; Bai, Y.; Edwards, A.; Colinge, J.; Bennett, K. L.; Gao, J.; Song, L.; Eschrich, S.; Superti-Furga, G.; Koomen, J.; Haura, E. B. *Nat. Chem. Biol.* **2010**, *6*, 291−299.
(12) Feitelson, M. A.; Arzumanyan, A.; Kulathinal, R. J.; Blain, S. W.; Holcombe, R. F.; Mahajna, J.; Marino, M.; Martinez-Chantar, M. L.; Nawroth, R.; Sanchez-Garcia, I.; Sharma, D.; Saxena, N. K.; Singh, N.; Vlachostergios, P. J.; Guo, S.; Honoki, K.; Fujii, H.; Georgakilas, A. G.; Bilsland, A.; Amedei, A.; Niccolai, E.; Amin, A.; Ashraf, S. S.; Boosani, C. S.; Guha, G.; Ciriolo, M. R.; Aquilano, K.; Chen, S.; Mohammed, S. I.; Azmi, A. S.; Bhakta, D.; Halicka, D.; Keith, W. N.; Nowsheen, S. *Semin. Cancer Biol.* **2015**, *35*, S25−S54.
(13) Tse, C.; Shoemaker, A. R.; Adickes, J.; Anderson, M. G.; Chen, J.; Jin, S.; Johnson, E. F.; Marsh, K. C.; Mitten, M. J.; Nimmer, P.; Roberts, L.; Tahir, S. K.; Xiao, Y.; Yang, X.; Zhang, H.; Fesik, S.; Rosenberg, S. H.; Elmore, S. W. *Cancer Res.* **2008**, *68*, 3421−3428.
(14) Zhu, Y.; Doornebal, E. J.; Pirtskhalava, T.; Giorgadze, N.; Wentworth, M.; Fuhrmann-Stroissnigg, H.; Niedernhofer, L. J.; Robbins, P. D.; Tchkonia, T.; Kirkland, J. L. *Aging* **2017**, *9*, 955−963.
(15) Lim, H.; Park, H.; Kim, H. P. *Biochem. Pharmacol.* **2015**, *96*, 337−348.
(16) Lee, Y. R.; Cho, H. M.; Park, E. J.; Zhang, M.; Doan, T. P.; Lee, B. W.; Cho, K. Y.; Oh, W. K. *Nutrients* **2020**, *12*, 1430−1446.
(17) Wang, R.; Yu, Z.; Sunchu, B.; Shoaf, J.; Dang, I.; Zhao, S.; Caples, K.; Bradley, L.; Beaver, L. M.; Ho, E.; Löhr, C. V.; Perez, V. I. *Aging Cell* **2017**, *16*, 564−574.
(18) Xu, M.; Palmer, A. K.; Ding, H.; Weivoda, M. M.; Pirtskhalava, T.; White, T. A.; Sepe, A.; Johnson, K. O.; Stout, M. B.; Giorgadze, N.; Jensen, M. D.; LeBrasseur, N. K.; Tchkonia, T.; Kirkland, J. L. *eLife* **2015**, *4*, e12997.
(19) Zhu, Y.; Tchkonia, T.; Pirtskhalava, T.; Gower, A. C.; Ding, H.; Giorgadze, N.; Palmer, A. K.; Ikeno, Y.; Hubbard, G. B.; Lenburg, M.; O'Hara, S. P.; Larusso, N. F.; Miller, J. D.; Roos, C. M.; Verzosa, G. C.; LeBrasseur, N. K.; Wren, J. D.; Farr, J. N.; Khosla, S.; Stout, M. B.; McGowan, S. J.; Fuhrmann-Stroissnigg, H.; Gurkar, A. U.; Zhao, J.; Colangelo, D.; Dorronsoro, A.; Ling, Y. Y.; Barghouthy, A. S.; Navarro, D. C.; Sano, T.; Robbins, P. D.; Niedernhofer, L. J.; Kirkland, J. L. *Aging Cell* **2015**, *14*, 644−658.
(20) Herber, B. E. *Plant Syst. Evol.* **2002**, *232*, 107−121.
(21) He, C. N.; Peng, Y.; Xu, L. J.; Liu, Z. A.; Gu, J.; Zhong, A. G.; Xiao, P. G. *Chem. Pharm. Bull.* **2010**, *58*, 843−847.
(22) Guo, W.; Dong, H.; Wang, D.; Yang, B.; Wang, X.; Huang, L. *Molecules* **2018**, *23*, 505−515.
(23) Liu, F.; Li, F. S.; Feng, Z. M.; Yang, Y. N.; Jiang, J. S.; Li, L.; Zhang, P. C. *Phytochemistry* **2015**, *110*, 150−159.
(24) Hoye, T. R.; Jeffrey, C. S.; Shao, F. *Nat. Protoc.* **2007**, *2*, 2451−2458.
(25) Slade, D.; Ferreira, D.; Marais, J. P. *Phytochemistry* **2005**, *66*, 2177−2215.
(26) Li, X.; Ferreira, D. *Tetrahedron* **2003**, *59*, 1501−1507.
(27) Cottyn, B.; Kollmann, A.; Waffo-Teguo, P.; Ducrot, P. *Chem. - Eur. J.* **2011**, *17*, 7282−7287.
(28) Baader, S.; Podsiadly, P. E.; Cole-Hamilton, D. J.; Goossen, L. J. *Green Chem.* **2014**, *16*, 4885−4890.
(29) Zaki, M.; Tebbaa, M.; Hiebel, M.-A.; Benharref, A.; Akssira, M.; Berteina-Raboin, S. *Tetrahedron* **2015**, *71*, 2035−2042.
(30) Garcez, F. R.; Garez, W. S.; Hamerski, L.; Miranda, A. C. D. M. *Quim. Nova* **2010**, *33*, 1739−1742.
(31) Zhang, G.; Shimokawa, S.; Mochizuki, M.; Kumamoto, T.; Nakanishi, W.; Watanabe, T.; Ishikawa, T.; Matsumoto, K.; Tashima, K.; Horie, S.; Higuchi, Y.; Dominguez, O. P. *J. Nat. Prod.* **2008**, *71*, 1167−1172.
(32) Yamauchi, S.; Sugahara, T.; Nakashima, Y.; Okada, A.; Akiyama, K.; Kishida, T.; Maruyama, M.; Masuda, T. *Biosci., Biotechnol., Biochem.* **2006**, *70*, 1934−1940.
(33) Cho, H. M.; Ha, T. K. Q.; Dang, L. H.; Pham, H. T. T.; Tran, V. O.; Huh, J.; An, J. P.; Oh, W. K. *J. Nat. Prod.* **2019**, *82*, 702−713.